

# New Wing Stroke and Wing Pitch Approaches for Milligram-scale Aerial Devices

Palak Bhushan and Claire Tomlin  
Dept. of EECS, UC Berkeley.

**Abstract**—Here we report the construction of the simplest transmission mechanism ever designed capable of converting linear motions of any actuator to  $\pm 60^\circ$  rotary wing stroke motion. It is planar, compliant, can be fabricated in a single step and requires no assembly. Further, its design is universal in nature, that is, it can be used with any linear actuator capable of delivering sufficient power, irrespective of the magnitude of actuator displacements. We also report a novel passive wing pitch mechanism whose motion has little dependence on the aerodynamic loading on the wing. This exponentially simplifies the job of the designer by decoupling the as of yet highly coupled wing morphology, wing kinematics and flexure stiffness parameters. Like the contemporary flexure-based methods it is an add-on to a given wing stroke mechanism. Moreover, the intended wing pitch amplitude could easily be changed post-fabrication by tuning the resonance mass in the mechanism.

## I. INTRODUCTION

Flapping wing microrobots [1]–[6] utilize insect wing kinematics to generate lift, which have periodic  $80^\circ$ – $150^\circ$  peak-to-peak wing stroke and approximately  $90^\circ$  peak-to-peak wing pitch amplitudes [7]. Most contemporary transmission designs use the mechanical advantage principle to amplify small actuator displacements [8] into large wing stroke rotations. This operating principle in conjunction with the small linear displacements involved demand a high resolution requirement on the fabrication methods used [9]. Moreover, due to the macro-scale mechanism design principle of rigid-links plus revolute-joints used, these are typically a multi-material design followed by 3D assembly. Here, inspired from [6], we use a resonant transmission instead to achieve large wing strokes which relaxes the resolution demand on the fabrication procedure used. We also design this resonant system to be planar and single-material for ease in assembly.

There is a  $90^\circ$  phase difference between the stroke and pitch in order to always maintain a positive wing angle-of-attack. For simplicity in fabrication all works in the milligram-size-scale only actuate stroke and achieve wing pitch passively by utilizing the  $90^\circ$  phase-lagged (with respect to stroke) aerodynamic loading on the wing together with a flexure joint of appropriate rotational stiffness near the wing leading edge and operate the system quasi-statically [7]. Not only is the flexure manufacturing elaborate involving aligned sandwiching of multiple laser cut layers [10], tedious design iterations occur due to the non-linear interdependency between flexure stiffness, wing pitch, wing shape and size caused by complex fluid dynamics. Different stiffness hinges needed to be tried for any changes made to the wing shape and to achieve

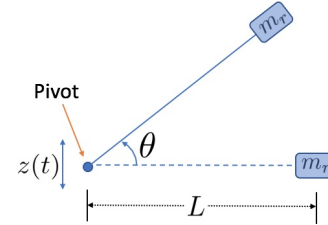


Fig. 1: Linearly driven torsional pendulum with linear excitation in the marked  $z$ -direction.

desired pitch. Here we use centripetal force as opposed to wing damping to produce fairly decoupled  $90^\circ$  phase-lagged wing pitch, and use better fatigue strength metals like steel as opposed to polymers [10]. This is also easier to manufacture and manually assemble because of a mostly single-material planar design.

## II. DESIGN

### A. Stroke mechanism physics

A simple pendulum is able to convert linear motion of the support to rotary motion of the mass. We use this idea and replace the restoring force due to gravity by a torsional pivot, thus creating a linearly driven torsional pendulum like the one shown in Fig. 1.

This linearly driven torsional pendulum is governed by

$$I_x \ddot{\theta} = -k_t \theta - b L_w^2 \dot{\theta} - b L_w \dot{z} \cos(\theta) - m_r L \cos(\theta) \ddot{z} \quad (1)$$

where the pivot is driven periodically as  $z(t) = z_{max} \sin(\omega t)$ , and thus  $\dot{z}(t)$ ,  $\ddot{z}(t)$  are known functions of time.  $m_r$  is the mass added at radial distance  $L$  for resonance,  $I_x = m_r L^2$  is the inertia of the rotating mass about rotation axis,  $k_t$  is torsional spring constant,  $L_w$  is the radial distance of the wing's effective center-of-pressure (c-p) from the pivot, and  $b$  determines the effective angular damping acting at  $L_w$ .  $\omega$  is chosen  $= \sqrt{\frac{k_t}{I_x}}$  for resonance. For a 100mg aerial device, assuming 3x average lift force  $\approx 1.5\text{mN}$  to be the peak force seen by each of the two wings, the damping factor  $b$  is chosen as

$$b = \frac{1.5 \cdot 10^{-3}}{L_w \omega \frac{\pi}{3} + z_{max} \omega} \quad (2)$$

to approximately mimic wing damping. Let us assume some representative values for the actuator displacement  $z_{max}$  and its frequency  $f$ , the resonant mass  $m_r$  and wing's  $L_w$ . For  $z_{max} = 0.8\text{mm}$ ,  $f \approx 200\text{Hz}$ ,  $m_r = 2\text{mg}$ , and  $L_w \approx 4.4\text{mm}$ ,

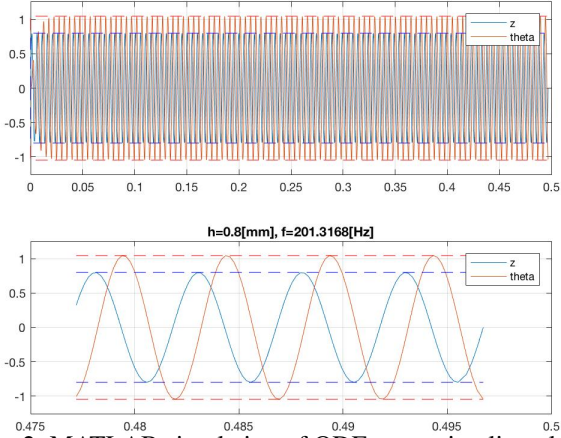


Fig. 2: MATLAB simulation of ODE governing linearly driven torsional pendulum. For the height  $z(t)$  of the pivot oscillating with amplitude of 0.8mm, an angular oscillation amplitude of  $60^\circ$  is achieved by the torsional spring.

MATLAB differential equation simulation yields the following working values for the rest of the parameters

$$L = 2.5\text{mm}, k_t = 20\mu\text{Nm} \quad (3)$$

in order to achieve stroke angle of  $\pm 60^\circ$  (see Fig. 2). Appropriately scaled values of  $f$  and  $m_r$  work as well. Note that the above is a simplified model capturing the basic idea of the transmission, and the actual transmission will have a more distributed resonant mass in contrast to the point mass  $m_r$ .

The inertial and elastic forces and torques of the order of 10mN and  $20\mu\text{Nm}$ , respectively, dominate over the damping forces and torques of the order of 1mN and  $5\mu\text{Nm}$  due to drag and lift in the proposed design. Thus, while designing for the stiffness of the springs, it is sufficient to just consider the inertial forces and torques which are given by  $F_{inertial} = m_r \omega^2 L \approx 8\text{mN}$ , and,  $T_{inertial} = F_{inertial} \cdot L \approx 20\mu\text{Nm}$ . Thus, an inertial torque of  $20\mu\text{Nm}$  acting on a  $k_t = 20\mu\text{Nm}$  torsional spring will cause an angular displacement of  $1\text{rad} \approx \frac{\pi}{3}\text{rad} = 60^\circ$ , just as desired.

### B. Compliant pivot

The compliant planar spring (see Fig. 3) is designed according to the method outlined in [6], [9] and laser cut from 301 stainless steel (see Table 1).

TABLE I: Steel spring specifications.

# parallel beams	16
Length of each beam	1mm
Beam width	0.1mm
Beam thickness	38um

### C. Pitch mechanism physics

The proposed wing pitching mechanism is driven with a periodic stroke angle externally (Fig. 4). We utilize the fact that centripetal forces are maximum at zero stroke (maximum stroke speed) and zero at extreme stroke angles (zero stroke speed) (Fig. 5). Wing is made using carbon-fiber veins and

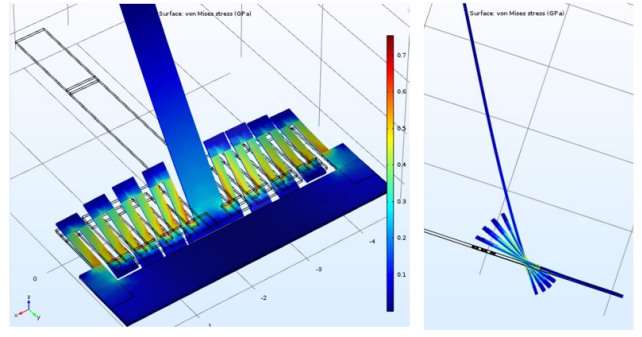


Fig. 3: Compliant pivot capable of large rotations with small stresses. x-axis is the pivot's rotation axis. This design achieves a rotation of  $60^\circ$  with an applied torque of  $T_x = -20\mu\text{Nm}$ . All the stresses during operation are well below 0.8GPa which cold rolled steel can withstand.

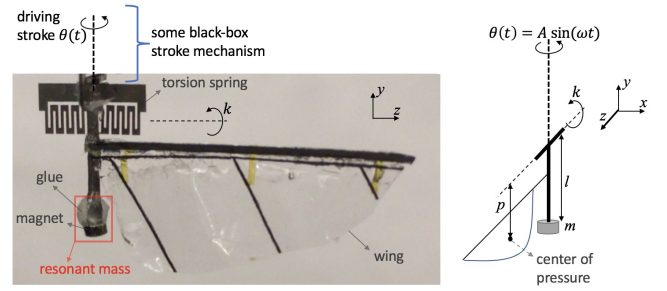


Fig. 4: (Left) Front view of the assembled pitch mechanism with 1mg steel spring and 0.4mg 15mm wing. (Right) Perspective view of the abstract mechanism in neutral wing stroke and neutral wing pitch position.

polyester membrane in a process similar to [6], [9], [11]. A  $m = 4\text{mg}$  magnet is glued at a distance  $l$  from the torsion springs rotation axis. System's motion is described by

$$ml^2 \ddot{\phi} = -k\phi + bL_w A \omega \cos(\omega t) p + ml \sin(\phi) (A \omega \cos(\omega t))^2 l \cos(\phi) \quad (4)$$

where distance  $p$  of the wings c-p from z-axis is estimated at 2.5mm, distance  $L_w$  from y-axis is estimated at 4mm, and  $b$  is the effective damping coefficient of the wing such that  $bL_w A \omega = 1\text{mN}$  to be approximately consistent with the peak aerodynamic force seen by the wing. During motion the spring is bent due to the torques caused by the radial centripetal forces in the xz-plane acting on the mass, and due to the aerodynamic force acting at wings c-p. Using ODE simulations in order to achieve  $\phi = \pm 45^\circ$  we select  $l = 5\text{mm}$  and  $k = 20\mu\text{Nm}$ , and use the same spring as before.

## III. EXPERIMENTS

To demonstrate the stroke mechanism we excite the transmission at 70Hz without a damper using an external linearly vibrating bench and observe the rotation amplitude possible.  $m_r$  is tuned to  $\approx 18\text{mg}$  to observe resonance. Fig. 6 shows amplitudes exceeding  $\pm 60^\circ$ , and a fixed axis of rotation, thus verifying our transmission design.

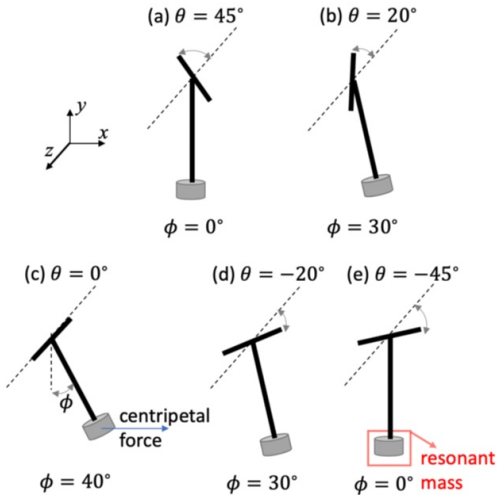


Fig. 5: Perspective view of the abstract mechanism while in motion from the positive extreme to the negative extreme stroke angle. These correspond to the last 5 snapshots in Fig.7.

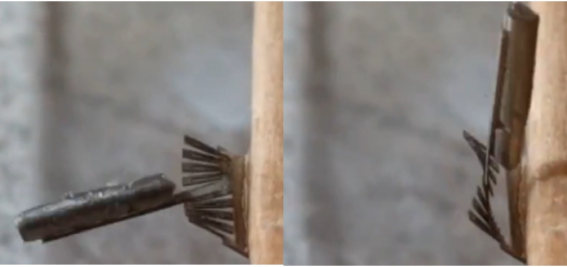


Fig. 6: Transmission excited via an external vibrating bench (seen in brown).

Next, the pitch mechanism is driven at  $\pm 45^\circ$  stroke and  $f = 70\text{Hz}$ . The resonant mass is tuned using glue and attaching smaller magnets till a decent wing pitch amplitude is observed (Fig. 7). From equation (4), the peak aerodynamic torque (2nd term) on the spring is estimated at  $bL_w A\omega p = 2.5\mu\text{Nm}$  and the peak inertial torque due to the mass (3rd term) is estimated at  $8\mu\text{Nm}$  portraying the dominance of inertial loading over aerodynamic loading. Other potential benefits of this design is it could support heavier wings and could be made to function in other mediums like water.

#### IV. CONCLUSION

We presented a resonant transmission mechanism that can amplify the periodic displacements of any actuator into large rotations. To achieve the complete wing kinematics we then designed a passive wing pitch mechanism than can be driven by the first stroke mechanism, and whose motion is additionally decoupled from the wing loading.

#### ACKNOWLEDGEMENTS

The authors are grateful to get support from Commission on Higher Education (award #IID-2016-005) and DOD ONR Office of Naval Research (award #N00014-16-1-2206). We would also like to thank Prof. Ronald Fearing for his help and insightful discussions.

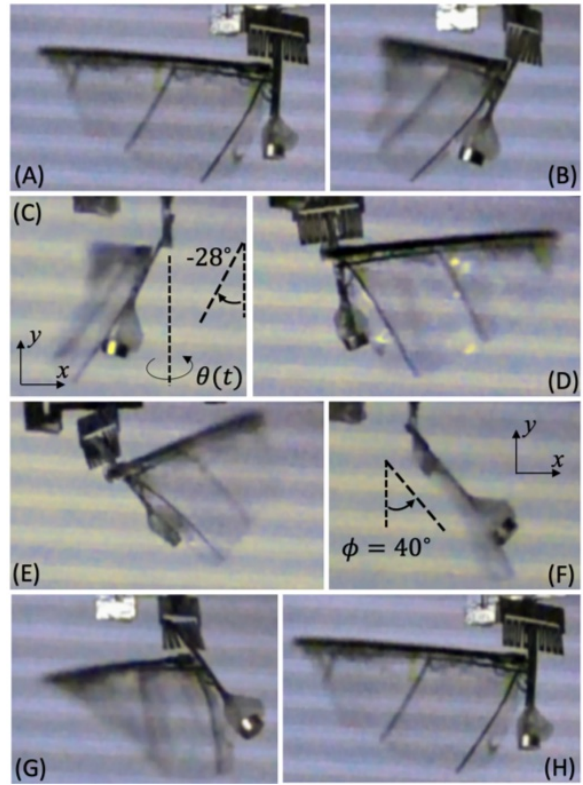


Fig. 7: Side view ( $xy$ -plane) of the mechanism while in motion for a complete wing stroke cycle, starting and ending at the negative extreme stroke angle. The last 5 snapshots (D-H) correspond conceptually to the 5 positions described in Fig. 5. Maximum wing pitch occurs at mid-stroke (see (F)), and zero pitch occurs at the 2 extreme strokes (see (A=H) & (D)).

#### REFERENCES

- [1] K. Ma, P. Chirattanon, S. Fuller, and R.J. Wood, "Controlled Flight of a Biologically Inspired, Insect-Scale Robot," *Science*, vol. 340, pp. 603-607, 2013.
- [2] X. Yan, Z. Liu, M. Qi, L. Lin, "Low Voltage Electromagnetically Driven Artificial Flapping Wings," *MEMS*, pp 1149-1152, Jan. 2016.
- [3] Z. Liu, X. Yan, M. Qi, Y. Yang, X. Zhang, L. Lin, "Lateral Moving of an Artificial Flapping-Wing Insect Driven by Low Voltage Electromagnetic Actuator," *MEMS*, pp 777-780, Jan. 2016.
- [4] X. Yan, M. Qi, and L. Lin, "Self-Lifting Artificial Insect Wings via Electrostatic Flapping Actuators," *Proceedings of 28th IEEE Micro Electro Mechanical Systems Conference*, pp. 22-25, Portugal, Jan. 2015.
- [5] Y. Zou, W. Zhang, and Z. Zhang, "Liftoff of an Electromagnetically Driven Insect-Inspired Flapping-Wing Robot," *IEEE Transactions on Robotics*, vol. 32, no. 5, October 2016.
- [6] P. Bhushan and C.J. Tomlin, "Milligram-scale Micro Aerial Vehicle Design for Low-voltage Operation," *IROS*, Madrid, Spain, Oct. 2018.
- [7] J. P. Whitney and R. J. Wood, "Aeromechanics of passive rotation in flapping flight," *J. Fluid Mech.*, vol. 660, pp. 197-220, 2010.
- [8] M. Karpelson, G-Y. Wei, and R.J. Wood, "A Review of Actuation and Power Electronics Options for Flapping-Wing Robotic Insects," *IEEE Int. Conf. on Robotics and Automation*, Pasadena, CA, May, 2008.
- [9] P. Bhushan and C.J. Tomlin, "Design of the first sub-milligram flapping wing aerial vehicle," *MEMS*, Seoul, South Korea, Jan. 2019.
- [10] R. Malka, A.L. Desbiens, Y. Chen, and R. J. Wood, "Principles of Microscale Flexure Hinge Design for Enhanced Endurance," *IROS*, Chicago, IL, Sept. 2014.
- [11] R. J. Wood, "Liftoff of a 60mg flapping-wing MAV," *IROS*, San Diego, CA, Oct. 2007.